Uncertainties in the atmospheric loading to ice-sheet deposition for volcanic aerosols and implications for forcing reconstruction

Chaochao Gao[1,2], Ya Gao[1,2]

[1]College of Environmental and Resource Science, Zhejiang University, Hangzhou 310058, China

[2]Zhejiang Provincial Key Laboratory of Organic Pollution Process and Control, Hangzhou 310058, China

Corresponding author: Chaochao Gao, gaocc@zju.edu.cn

Key Points:

- The existing the stratospheric volcanic aerosol loading to ice core sulfate deposition (LTD) factors is comparatively reviewed
- New set of LTD is obtained using the most comprehensive ice core observations of Tambora debris
- Uncertainties in LTD is estimated using Monte Carlo sampling of selected number of cores and cross-eruptions
- Results indicate small uncertainty due to ice core sampling but potentially large uncertainty among eruptions

Abstract

Volcanic radiative forcing reconstruction is an important part of paleoclimate simulation and attribution efforts, and the conversion factor used to transfer ice core-based sulfate observation into stratospheric volcanic aerosol loading (LTD factor) is critical for such reconstruction. A Pinatubo-based LTD was proposed and adapted in the CMIP5 and CMIP6 volcanic forcing, under the assumption that all tropical eruptions follow the same atmospheric transport and deposition pattern. This study revisits the LTD factor using a large collection of polar ice core records of Tambora deposition and a Monte Carlo sampling model. A new set of LTDs with associated uncertainties are obtained, which is in approximate with our previous Pinatubo-based LTD estimation in Greenland, while corrects the bias of over-representing the west Antarctic. The uncertainties revealed from the Monte Carlo simulation suggest that, difference in the ice core abundance only introduce limited uncertainty in LTD for individual eruption, once reach a certain threshold (about 15 in Greenland and 20 in Antarctic). The comparison of Southern Hemispheric LTD among Tambora, Agung, and Pinatubo suggests that, the conversion factor may vary for individual eruption. Results obtained from this study may ease our conventional proneness to use as much ice core observations as available to estimate icecap volcanic deposition, while emphasize the importance to build a distribution of the LTD ideally for eruptions with different size and locations. Meanwhile, the estimated sets of Tambora-based LTDs could serve as a compromising choice in future volcanic forcing reconstruction work, especially when Tambora is utilized as a reference

1 Introduction

Volcanic eruption is an important cause of natural climate variability, and polar ice preserves the nature, including timing and magnitude of the historical eruptions long before human observation. For the ice-core volcanic achieves to be utilized in climate models, however, one has to convert the amount of deposited volcanic sulfate in the ice caps back to the stratospheric sulfate mass loading. This inverse reconstruction may introduce substantial uncertainties, due to the discrepancy in ice core volcanic deposition measurements and perhaps more importantly, the limitations in the conversion factor to transfer the ice core observation into the stratospheric volcanic sulfate loading (hereafter referred to as the LTD factor).

Previous studies have tried to derive the LTD factor combing different lines of observation and model simulations. Clausen and Hammer (1988) pioneered the use of bomb test debris to calculate the LTD factor for Greenland ice cores, based on the assumption that the transport and deposition of volcanic aerosols are analog to those of bomb test debris on a large scale. Cole-Dai and Mosley-Thompson (1999) utilized the ratio between Pinatubo depositions in six South Pole ice cores and its atmospheric aerosol loading to linearly convert the ice core volcanic signals to their stratospheric loadings, assuming similar transport and deposition pattern for all tropical eruptions. Crowley (2000) and Ammann et al. (2003) applied the same approach but different reference events of Krakatau and Tambora, respectively, as the empirical scaling.

Crowley (2000) applied an additional 2/3 power dampening factor, to account for the self-limiting effects of sulfate aerosols for the eruptions larger than Pinatubo (Pinto et al., 1989).

In recent years, the coupled chemistry-climate models have been utilized to estimate the conversion factors. Toohey et al. (2013) tested the assumption of directly proportional relationship between the stratospheric volcanic aerosol loading and ice sheet deposition using the MAECHAM5-HAM aerosol-climate model, and the model results show excellent spatial correlation but 4-5 times larger deposition fluxes compared with ice core observations. Marshall et al. (2018) further calculated the atmospheric burden to ice core deposition conversion factors (BTD) using MAECHAM5- HAM and three additional coupled chemistry-climate models, and found BTD to differ by a factor of five for Northern Hemisphere and by an even larger factor of 15 for Southern Hemisphere among the models. The results suggest that the current aerosol-climate models may not up to giving the accurate estimation of the conversion factors for volcanic clouds.

The conversion factors derived in Gao et al. (2007) have been utilized in the ice-core-based volcanic forcing reconstruction of Gao et al. (2008) and Sigl et al. (2015). Gao et al. (2008) reconstructions has been widely used in the CMIP5 models; and Sigl et al. (2015) reconstruction, together with Toohey and Sigl (2017), has been recommended for the CMIP6 model simulations. However, only six out of the 19 Antarctic records used in Gao et al. (2007) cover the vast regions of inner and east continent, and the accumulation rates in the west Antarctic cores are on average one order of magnitude larger than the east Antarctic cores. The uneven distribution of the ice core records, coupled with the large spatial variability of volcanic deposition (Zielinski et al., 1995; Traufetter et al., 2004; Gautier et al., 2016) may have biased the conversion factors.

The new high-depth-resolution volcanic sulfate records from East Antarctic (Sigl et al., 2014), and the coupled chemistry-climate modeling studies of Tambora or Tambora-size eruptions, make the revisit of the conversion factor and evaluation of its uncertainties possible. It is the aim of this study to derive a new set of conversion factor and estimated the associated uncertainties, based on a comprehensive collection of ice core records for Tambora volcanic depositions and a Monte Carlo random sampling model. The set of conversion factors and uncertain estimates will be consistent for Antarctic and Greenland ice core data in terms of methodology, and can be compared both with the multimodal-derived NH_BTD & SH_BTD factors (Marshall et al., 2018) and other ice-core-derived factors in a more systematic framework.

2 Data and Methods

By measuring the amount of volcanic sulfate that was deposited in polar ice sheets, in theory one could an inverse calculation of the LTD factor as the following equation:

$$LTD = L \div D \quad (1)$$

where L is the stratospheric volcanic mass loading (usually in Tg of SO_2 or sulfate aerosols); D is the icecap average of the volcanic deposition measured in each ice core record (usually in kg/km^2 of none-sea-salt SO_2^{4-}).

2.1 Volcanic deposition in polar ice cores

Calculation of the volcanic deposition, if start with the raw ice core measurements, involves multiplication of ice or snow concentration (c), ice or water equivalent density (d), and the deposition thickness (h) as shown in equation (2)

$$D = c \times d \times h \quad (2)$$

In this study we maintain the original ice core records used to derive the Pinatubo-based LTD, which in Greenland includes six PARCA cores (Mosley-Thompson et al., 2003), 12 cores from Clausen and Hammer (1988), and 6 cores original to Gao et al. (2007). Therefore, the volcanic depositions for selected events are obtained directly from these records. In addition, we also include two northern Greenland cores – NEEM2011S1 and Tunu2013 (Sigl et al., 2015) in the calculation. For these two records, we apply the same volcanic signal extraction procedure as Gao et al. (2007), that is we identify the volcanic signals by applying a high-pass loess filter remove the influence of background concentration and extract the peaks that exceed twice the 31-year absolute running median. Table 2 lists the general information of these Greenland ice cores, and Figure 1 shows the site map and Tambora volcanic deposition of these ice cores. The addition of NEEM2011S1 and Tunu2013 significantly improved the sampling coverage of the low-accumulative Northern Greenland.

In Antarctic, we nearly double the number of ice-core records from the 17 in Gao et al. (2007) to 32 by including the annually dated WDC06A core from West Antarctic and 14 additional AVS-2K cores mainly from East Antarctic (Sigl et al., 2013 & 2015). Table 3 lists the information and Figure 2 shows the location and average accumulation rate of these Antarctic ice cores. Same procedure is applied to the WDC06A and AVS-2K cores, so that all the ice core volcanic depositions are obtained with the same criteria.

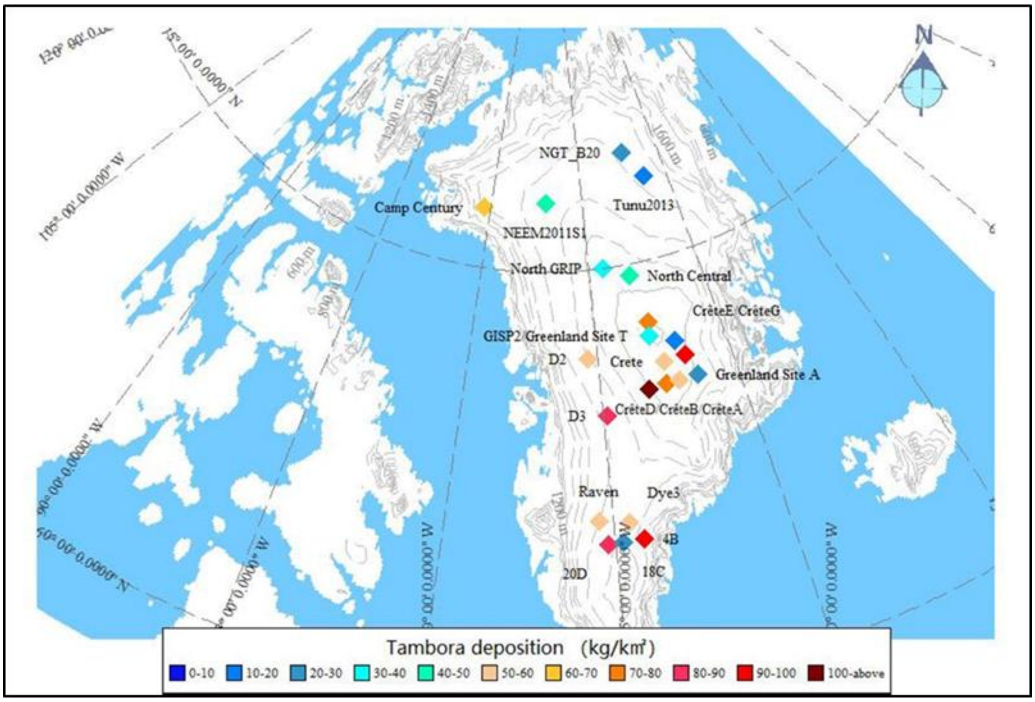

Figure 1. Location and Tambora volcanic deposition of the Greenland ice core records listed in Table 3.

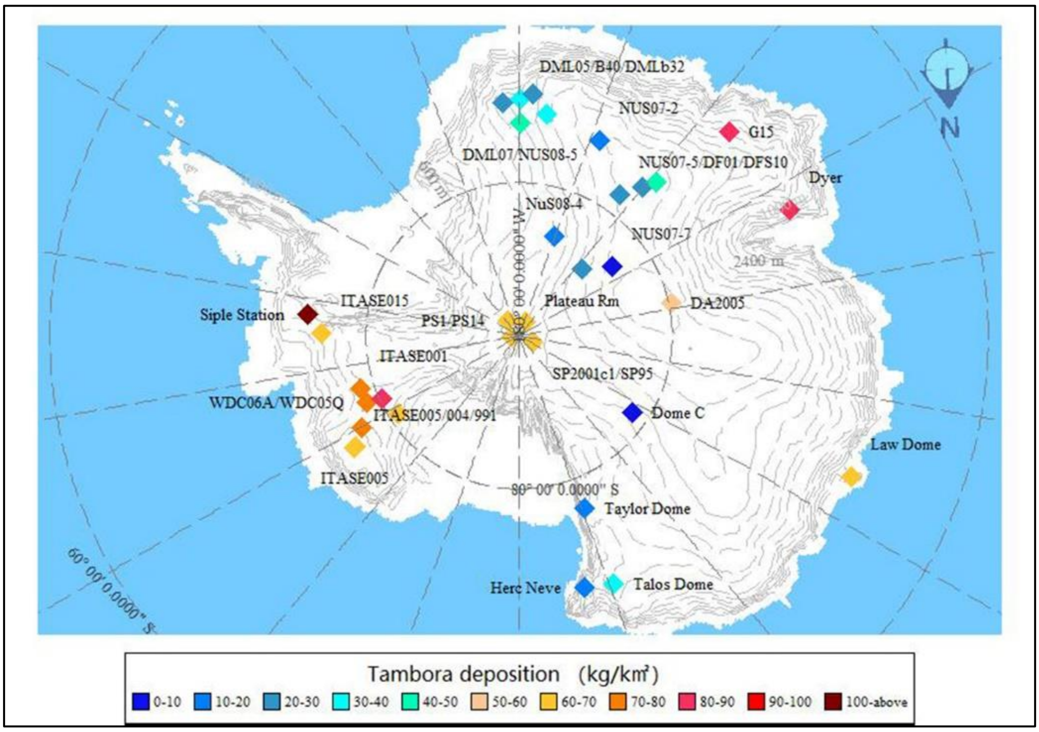

Figure 2. Location and Tambora volcanic deposition of the Antarctic ice core records listed in Table 3.

2.2 Calculation of the LTD factor

The 1815 Tambora eruption in Indonesia is chosen as the representative event to calculate the LTD factor, because its characteristics are relatively well known and the signals are detected in almost all ice core records. We also calculate the LTD factor of the 1963 Agung and 1991 Pinatubo eruptions, because they are the two recent events with comparable magnitudes and the latitudinal location of Agung is very close to Tambora (Figure 3).

We calculate the ice sheet mean deposition by taking the simple average of all records without consideration of their geological location and distribution, and in Greenland the simple-average Tambora deposition flux is 57 kg km^{-2}. For Antarctic, we take one step further by multiplying the average deposition of West Antarctic Peninsula and East Antarctic with 0.2 and 0.8, respectively, to reflect the size difference of these two areas (Sigl et al., 2015). The LTD factor for the selected three events are obtained following equation (1).

2.3 Monte Carlo random sampling of the ice core records and uncertainty estimation of the LTD factors

We retrieve the volcanic sulfate signals in 54 records, including 22 from Greenland and 32 from Antarctic ice cores, which we believe is the most comprehensive ice core - based observation (Table 2 & 3). The Tambora volcanic deposition flux varies as large as one order of magnitude among cores in both Greenland and Antarctic (Figure 1 & 2). It is therefore crucial to include a representative number of ice core observations in the analysis, and estimate the threshold of the representative number and the uncertainties in the associated LTD factors.

We conduct Monte Carlo random sampling of the volcanic records with varying ice core numbers, for each selected event in Antarctic and Greenland. This process is repeated 10,000 times to build a random distribution for the average Antarctic or Greenland volcanic deposition, against which the associated LTD factor for individual event is calculated by dividing the estimated magnitude of total stratospheric sulfate aerosol loading by the average icecap. The threshold of the representative ice-core-number and the uncertainties in the LTD factor, for example for Tambora and Laki eruptions, are estimated by the converging rate of the distribution.

2.4 LTD factors obtained from other sources

2.4.1 LTD factors obtained from the bomb test observations

A serial nuclear bomb tests were conducted from 1945 until 1980. In particular, the U.S. conducted two tests in the Pacific sites of Bikini (11° 35′ N 165° 23′ E, in 1952 CE) and Enewetak (11° 30′ N 162° 15′ E, in 1954 CE) during one of the most active period 1954-1958 CE (Bennett, 2002), and the location of these two test sites are in close latitudinal approximation of the Pinatubo (Figure 3). The explosion columns of these bomb tests are 20 km high and characterized by near instantaneous release and global dispersal of the volatile mass. The stratospheric residence time of the radionuclides is about 1-3 years, resembling the stratospheric residence time of the volcanic aerosols (Bennett, 2002; Robock, 2000).

Radioactive debris from the bomb tests were transported to polar ice sheets and preserved in the ice, and can be identified by total β activity examinations. Clausen and Hammer (1988) measured both the Tambora volcanic deposition and the total β activity of the 1952-54 tropical Pacific bomb tests in 16 Greenland ice cores, serving as the base for verification of the methodology.

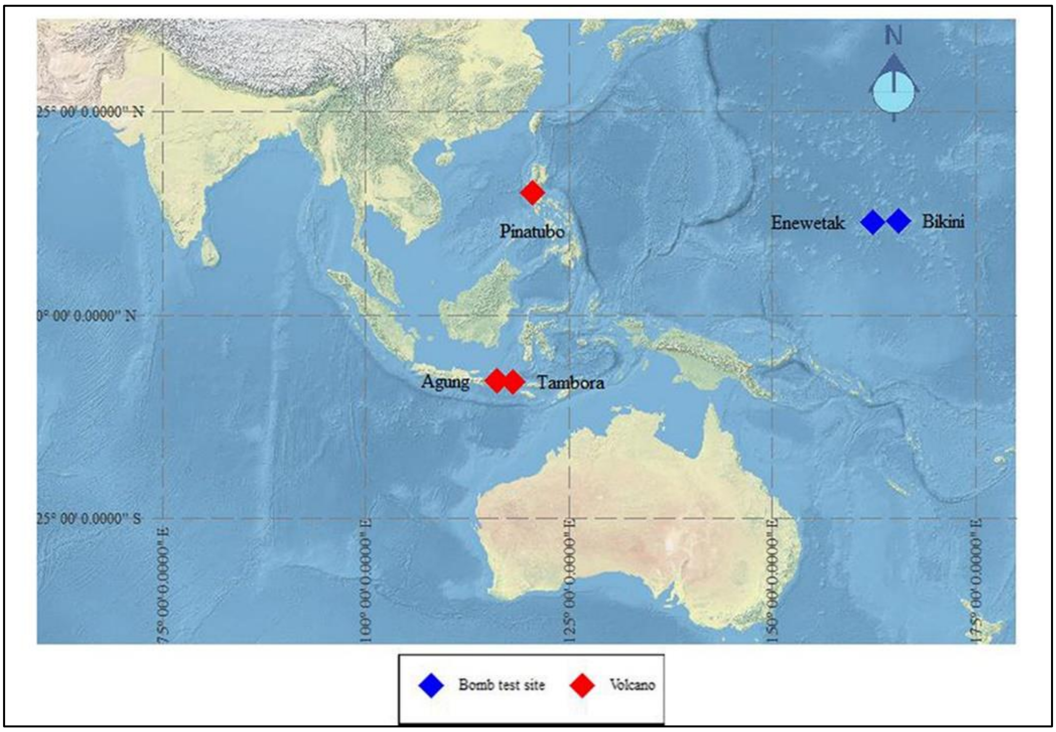

Figure 3. Location of the Pinatubo, Agung, and Tambora volcano sites (red diamonds), and the 1952-54 US bomb test site sites of Enewatak and Bikini (blue diamonds).

2.4.2 LTD factors obtained from model simulations

Toohey et al. (2013) calculated the deposition efficiency (i.e., the ratio between the hemispheric maximum stratospheric aerosol loading and the volcanic sulfate flux in Greenland or Antarctic), for the MAECHAM5-HAM aerosol-climate model. The model ensemble conversion factor for a Tambora - size eruption is 0.2×10^9 km^2 for both Greenland and Antarctic, regardless of the season.

Marshall et al. (2018) compared the Tambora volcanic sulfate deposition in four global aerosol-climate models, i.e., MAECHAM5- HAM, CESM1-WACCM, SOCOL-AER, and UM-UKCA, to that in ice core observations and calculated the burdening-to-deposition factors (hereafter referred to the original reference as

NH_BTD and SH_BTD). These BTD values, together with that from Toohey et al. (2013) are listed in Table 1, and serve as reference results for the uncertainty evaluation for the ice-core-based LTD factors.

3 Results and Discussions

3.1 Uncertainties in the existing conversion factors

Clausen and Hammer (1988) obtained the first sets of bomb test-based conversion factor for Greenland using the United Nations Scientific Committee on the Effects of Atomic Radiation 1982 Report (UNSCEAR1982, hereafter referred to as L_β-1982, Table 1). Gao et al. (2007) revisited the calculation with the updated UNSCEAR (2000) report, and used only the fission yields in stratosphere to mimic the volcanic sulfate loading. The obtained conversion factor (hereafter referred to as L_β-2000, Table 1) differ from the original L_β-1982 by a factor of two for the low NH latitude bomb tests, because about half of the fission ends up in the stratosphere.

Using the satellite observations of the atmospheric Pinatubo aerosol loading and 19 ice core depositions records in Antarctic, Gao et al. (2007) also calculated the conversion factor for Antarctic ice core-derived volcanic signals (hereafter referred to as L_p). Combining the Pinatubo-observation derived factors for Antarctic and the bomb-test derived factors for Greenland, Gao et al. (2007) obtained the conversion factor $(1.0\pm0.25)\times10^9$ km^2 (Table 1) to calculate the stratospheric sulfate aerosol loadings for tropical eruptions. Toohey and Sigl (2017) repeated the calculation for Antarctic using an updated set of ice core records (Sigl et al. 2015), and result is 35 %-50 % larger than that in Gao et al. (2007) (Table 1). Besides the difference in the ice core dataset, the two studies also used different methods to calculate the icecap mean volcanic depositions: instead of the simple arithmetic mean of local averages in Gao et al. (2007), Toohey and Sigl (2017) took the area-size into consideration and applied a weighting of 20/80 for West Antarctic and East Antarctic. Both may have contributed to the difference in the LTD values.

Marshall et al. (2018) found that, the model results differ significantly both among themselves and from the observation, in the magnitude and spatiotemporal pattern of the volcanic depositions. The resulting burdening-to-deposition factors (hereafter referred to the original reference as NH_BTD and SH_BTD, Table 1) ranges from 0.19×10^9 km^2 (in MAECHAM5- HAM) to 0.97×10^9 km^2 (in UM-UKCA), differ by a factor of 5 for Greenland ice records; and ranges from 0.19×10^9 km^2 (in MAECHAM5- HAM) to 2.91×10^9 km^2 (in UM-UKCA), differ by a factor of 15 for Antarctic ice records. Model results also show significantly less deposition in Antarctic than in Greenland. The multimodal-average NH_BTD and SH_BTD is 0.42×10^9 km^2 and 1.27×10^9 km^2, suggesting substantially asymmetric hemispheric transport and deposition of volcanic aerosols. The multimodal-average NH_BTD is close to our previous GISS model E simulations of the Tambora and Pinatubo depositions (Gao et al., 2007), whose resulting conversion factor is 0.46×10^9 km^2 for Pinatubo and 0.55 ×10^9 km^2 for Tambora, respectively (Table 1).

Toohey et al. (2013) found that the deposition efficiency was not linear but varied as a function of the eruption seasonality and magnitude. Taking the January eruptions for example, the deposition efficiency in Greenland increases gradually from about 4×10^{-9} km^{-2} for a half – Pinatubo - size eruption to 5×10^{-9} km^{-2} for a Tambora - size eruption, then declines slightly as the eruption size increase further. In Antarctic, the deposition efficiency stays the same for Pinatubo - or smaller - size eruptions, then starts to decline as the eruption size increases.

In summary, the conversion factors obtained in different studies contain large uncertainties. Some of the uncertainties are systematic, likely associated with the methodologies applied to derive the factor. For example, climate models tend to give small conversion factor due to the large poleward transport of stratospheric aerosols. Without proper area-weighting, the Antarctic-mean deposition maybe overestimated due to the disproportionally-dense ice core sampling in the high-accumulative West Antarctic Peninsula. Others are more specific and therefore difficult to evaluate. For example, the specific transport and deposition characteristic of individual eruptions, uncertainties in the volcanic deposition from core to core and from event to event, uncertainties also in ice core signal measurements. A common compromising assumption of existing studies is that all tropical eruptions following the same atmospheric transport pattern, whistle model simulations suggest eruption location, magnitude, and seasonality may have significant influence on the hemispheric partitioning and transport of volcanic aerosols. The potential influence of eruption characteristics on the conversion factor is simply unknown.

3.2 New LTD estimated with Tambora ice core records

The April 1815 eruption of Tambora (8.25° S, 118.00° E; Figure 3) released 60 - 80 Tg of SO_2 into the stratosphere, making it one of the largest explosive eruptions in the Common Era (Self et al., 2004; Gertisser et al., 2012). It is also the most widely studied eruption in terms of ice core observation, model simulation, proxy reconstruction, and climatic and socioecological aftermaths assessment (Luterbacher and Pfister, 2015; Raibie et al., 2016; Gao et al., 2017; Brönnimann et al., 2019).

Due to its explosive nature and large magnitude, Tambora volcanic deposition is widely observed in the polar ice sheets and used as the first order reference layer for ice core dating. The composites, after correcting for area-difference, show relatively similar sulfate deposition in Greenland (57 kg km^{-}2) and Antarctic (47 kg km^{-2}). This suggests that the hemispheric partition of Tambora sulfate aerosols is probably symmetric. Therefore, we take low size estimation of Tambora eruption, i.e., 60 Tg SO_2 as the total amount of sulfate gases injected into the stratosphere and divide the values equally into each hemisphere. This results in 61Tg of sulfate aerosols (assuming 75wt. % H_2SO_4 in water) in each hemisphere, respectively. The obtained ratio between the stratospheric sulfate loading and the average amount of sulfate deposited on each ice sheet for Greenland (hereafter referred to as NH-LTD_T) is 1.07×10^9 km^2 and for Antarctic (hereafter referred to as SH-LTD_T) is 1.29×10^9 km^2.

3.3 Characteristic of LTD_T due to different ice-core sampling

Toohey and Sigl (2017) suggested that the uncertainties in the conversion factor are composed of systematic uncertainties, static errors that potentially causing global bias in forcing estimation, and random differences that are specific to individual volcanic events or forcing reconstruction. The LTD_T values are subject to systematic uncertainties, for example, uncertainty in the estimation of stratospheric sulfate aerosol injection will directly influence the LTD_T values and the associated forcing reconstructions. If we apply the larger value of existing estimation 80 Tg SO_2, then NH-LTD_T and SH-LTD_T becomes 1.65×10^9 km^2 and 1.72×10^9 km^2, respectively

The random uncertainties are commonly associated with the variation of volcanic aerosols dispersion from case to case, and the finite sampling of ice cores through time. We therefore repeat the LTD_T calculations for finite sampling of ice cores, by applying the Monte Carlo random sampling with various sample sizes (Table 3) to build a distribution range and associated probability (Figure 4). The results show that, the distributions of LTD_T with different ice-core sample sizes are approximately normal, with slightly longer tails toward the right (Table 4). Therefore, we could use the mean (μ) and standard deviation (σ) to characterize the LTD_T values.

First of all, the distribution of differently-sampled LTD_T largely overlap with each other. The NH-LTD_T and SH- LTD_T values derived from the full set of Greenland and Antarctic ice core observations also lie very close to the mean of the Monte Carlo simulated distributions (Figure 4). Both results suggest the robustness in the estimated mean value w.r.t the sampling of ice cores. Secondly, the kurtosis decreases as we increase the sampling size, suggesting convergence of the LTD_T values, in another word, reduction of the uncertainties as the number of ice core records increases (Figure 4).

The convergence of LTD_T values within $\mu\pm\sigma$ suggests, albeit from only limited case comparison, that LTD_T is likely to contain limited uncertainties with respect to the ice cores, once the number of records reaches certain threshold. The threshold, judged from a compromising consideration of the convergence in the LTD_T values and the limited number of ice core observations for most volcanic events, is about 65% in terms of the percentage or 14 Greenland and 20 Antarctic ice core records, respectively (Table 4).

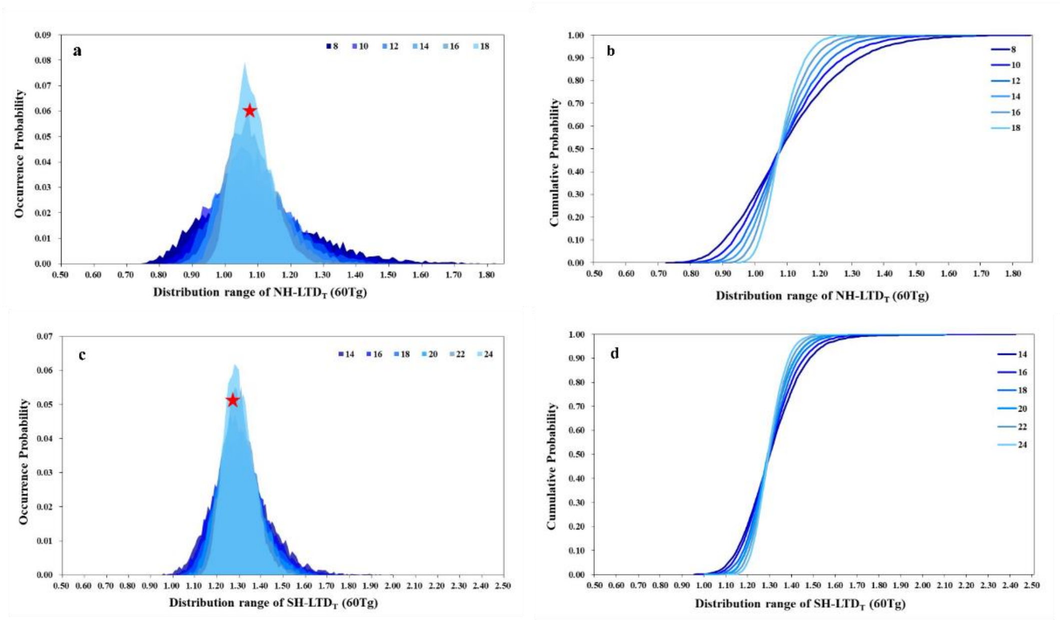

Figure 4. (a, c) Distribution of NH-LTD$_T$ and SH-LTD$_T$ estimated by Monte Carlo random sampling of selected number of ice core records; and (b, d) the corresponding cumulative occurrence probability. The red star in panel a and c represents the NH-LTD$_T$ and SH-LTD$_T$ values estimated with the full set of available ice core records.

3.4 Comparison of SH-LTD among Pinatubo, Agung, and Tambora based estimations

The value of NH-LTD$_T$ (1.08±0.056) is in general agreement with the Pinatubo-based conversion factor L_P for Greenland (Gao et al. 2007; Table 1), while SH-LTD$_T$ (1.29±0.066) is 29 % larger than L_P for Antarctic. The database used to derive SH-LTD$_T$ are composed of 18 records used in the original Gao et al. (2007, hereafter referred to as GC07) estimation and 14 records used in Sigl et al. (2015, hereafter referred to as MS15) reconstruction. Figure 5 shows the latitudinal and longitudinal location, accumulation rate, and Tambora sulfate deposition of these two group of records, from which we can see that all of the MS15 ice cores except WDC06A and WDC05Q are located in inland East Antarctic within74-84° S latitude band. The mean accumulation rate of the MS15 ice cores is 0.068 meter per year, only one third of that for GC07 cores (0.20 m/a). As a result, the average Tambora sulfate deposition flux is about sixty percent of the GC07 average deposition. In another word, the high-cumulative west Antarctic was over represented in L_P calculation (Gao et al., 2007) and this may help to explain why it is smaller than SH-LTD$_T$

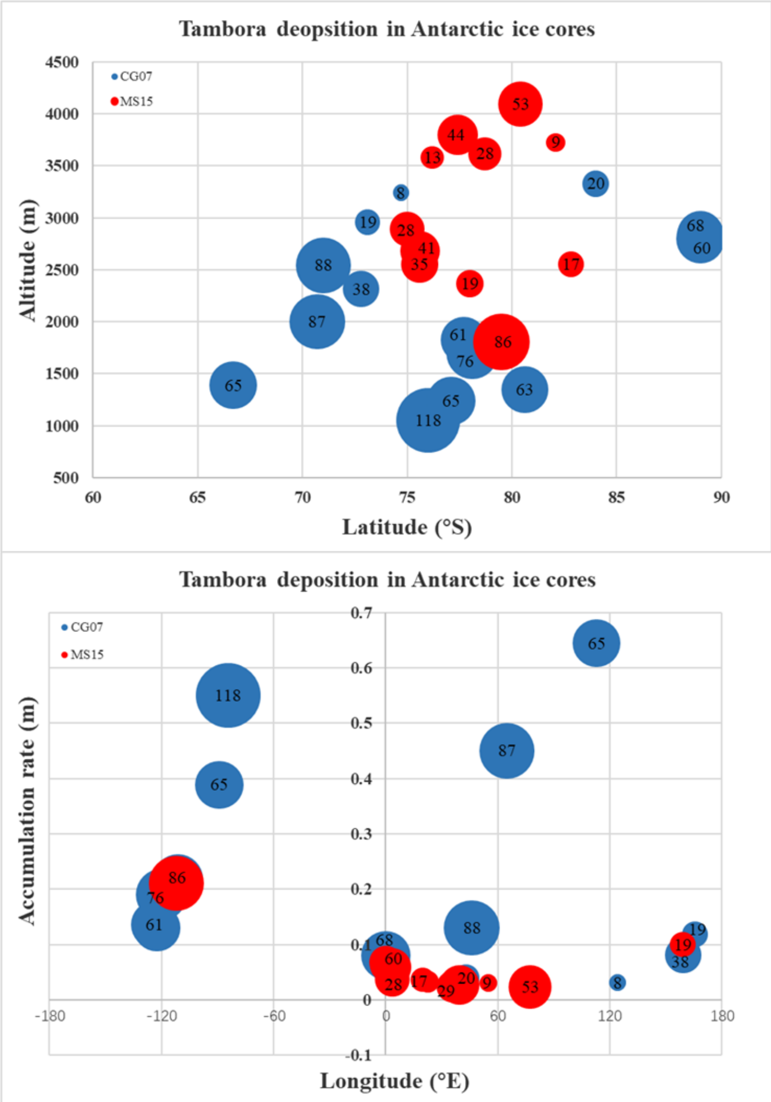

Figure 5. Difference in the Tambora deposition between the Antarctic ice cores used in the Gao et al. (2007, referred to as CG07 and represented as the blue bubbles) and Sigl et al. (2015 referred to as MS15 and represented as the orange bubbles) reconstruction. The size of the bubbles and values inside each bubble indicates the deposition (kg/km^2). Some ice core records overlap with the others therefore are not visible in the figure.

To update the comparison, we apply the same Monte Carlo analysis for the Pinatubo eruption using 18 available ice core records and the 1963 Agung eruption using 24 ice core records (Table 3). The resulting conversion factor SH-LTD$_P$ and SH-LTD$_A$ with the full set of available ice core records is 1.87×10^9 km^2 and 0.95×10^9 km^2, respectively. Monte Carlo random sampling of the selected percentages of ice core records suggests the distribution range of SH-LTD$_P$ as 1.67±0.09×10^9 km^2 (Table 4), therefore larger than that of Tambora assuming 60Tg SO_2 injection. On the other hand, if we assuming 80Tg SO_2 as the eruption size of Tambora, SH-LTD$_T$ becomes

$1.74 \pm 0.09 \times 10^9$ km^2, largely overlap with SH-LTD$_P$ (Figure 6). Similar Monte Carlo simulation suggests the distribution range of SH-LTD$_A$ as $0.92 \pm 0.04 \times 10^9$ km^2.

The comparison among the three eruptions suggests the possibility that, the LTD factor may vary for individual eruption, depending on the volcano location, eruptive magnitude, etc. Agung volcano lies close to Tambora, while its eruption size is much smaller in terms of the SO_2 injection, therefore more sulfate aerosols may have stayed in the atmosphere longer and reached the ice sheets. Besides, observations indicate 2SH:1NH dispersion of the Agung aerosols. Although we have accounted for the hemispheric partitioning difference in calculating the stratospheric loading, disproportionally more Agung debris could have reached Antarctic and dwarf the conversion factor. Pinatubo is about 20- degree north of Tambora (Figure 3), but observations show that the volcanic cloud disperse more or less evenly between the two hemispheres. The dispersion and transport of individual volcanic cloud are therefore difficult to anticipate, and their potential influence on LTD is hard to quantify. On the other hand, the Antarctic cores with the highest Tambora deposition, i.e., Siple Station, Dyer, and G15, do not have record for Pinatubo deposition, therefore probably reduces the Antarctic average Pinatubo deposition and increases the conversion factor. If we remove the three ice core records from the Tambora simulation, the SH-LTD$_T$ (60Tg SO_2 injection) value would increase from $1.08 \pm 0.056 \times 10^9$ km^2 to $1.44 \pm 0.077 \times 10^9$ km^2. The variation in ice core depositions therefore introduce another layer of uncertainty.

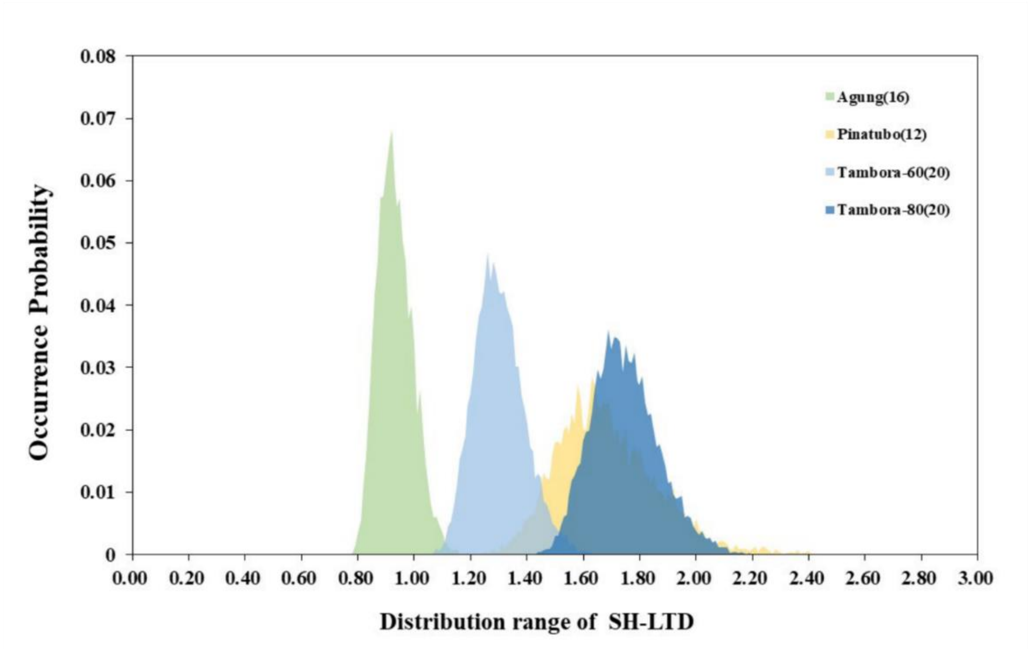

Figure 6. Distribution of SH-LTDs estimated by Monta Carlo random sampling of the threshold number of ice core records (i.e., ~65%) for Agung, Pinatubo,

and Tambora. The light and dark blue shadings represent the distribution of $SH\text{-}LTD_T$ assuming a Tambora SO_2 injection of 60Tg and 80Tg, respectively.

3.5 Comparison with the conversion factors obtained from other sources

For Southern Hemisphere, none of the four aerosol-climate model simulated conversion factors ($SH\text{-}BTD_T$, Table 1) fall within the range of the newly obtained $SH\text{-}LTD_T$ (Figure 7), despite the fact that the 4 model-mean $SH\text{-}BTD_T$ appear to be in good agreement. $SH\text{-}BTD_T$ itself varies among the four models by up to a factor of 15 (Marshall et al., 2018). CESM-WACCM derived $SH\text{-}BTD_T$ is the closest to the ice-core derived SH-LTDs, especially that of Pinatubo. In Northern Hemisphere, the UM-UKCA derived $NH\text{-}BTD_T$ fall within the range of $NH\text{-}LTD_T$. Both of them, nevertheless, have BTD_T of the other hemisphere way off the LTD_T ranges. The conversion factor for Tambora and Pinatubo based on previous GISS simulations (Gao et al. 2007) are also much smaller than their LTD counterparts (Figure 7), echoing the general model tendency to transport more flux toward polar regions.

Different from the symmetric partition assumption based on ice core observations, all four aerosol-climate models tend to keep more Tambora volcanic sulfate aerosols in Southern Hemisphere (Table 5 and Figure 11 in Marshall et al., 2018), likely as a result of the 8.25° S latitudinal location of the volcano. None of the model simulated volcanic deposition in ice sheets is in close agreement with ice core observation, therefore it is also difficult to match ice core observations with individual model to judge model performance or confirm model-proxy consistency in the conversion factors.

We also compare $NH\text{-}LTD_T$ with the Gao et al. (2007) estimation of conversion factor using the radioactive debris deposition from the nuclear bomb tests (L_β-2000). As we can see from the pink shading in Figure 7, the $NH\text{-}LTD_\beta$ values, either symmetric or 2NH:1SH partitioning, are smaller than $NH\text{-}LTD_T$. The L_β-2000 value under the 2NH:1SH partitioning assumption is, however, close to $SH\text{-}LTD_A$. Given that both vlaues are based on the ice core observations of the same hemisphere and assuming a two third hemispheric partitioning of the event debris, the closeness in results confirms that the LTD factor may vary depending on eruption magnitudes and locations.

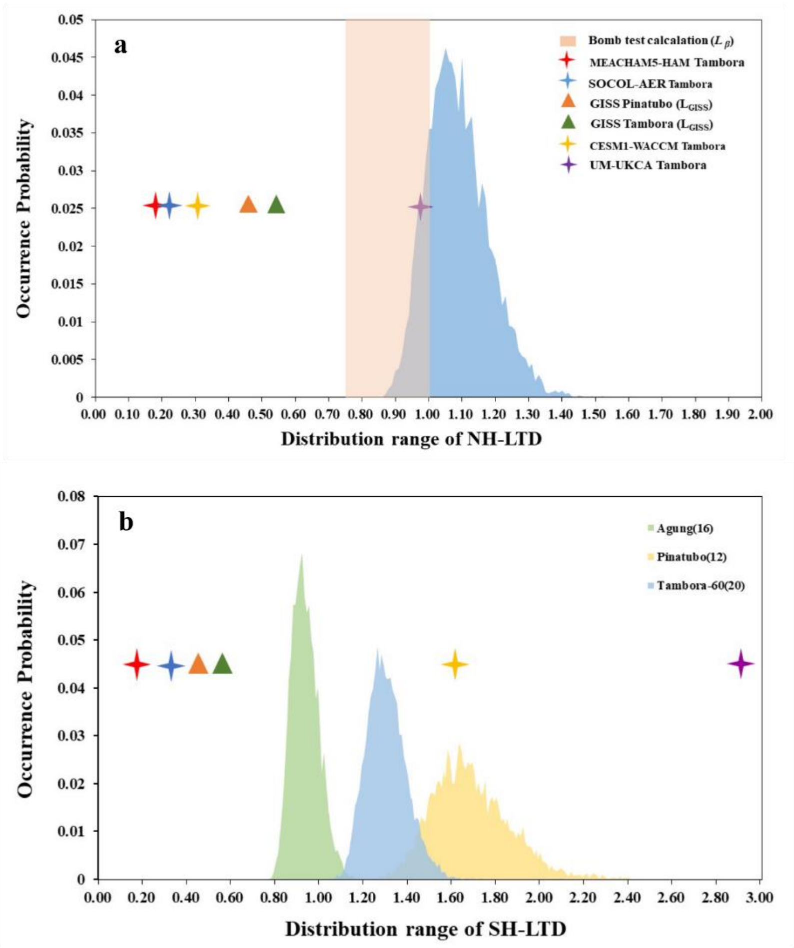

Figure 7. Distribution of NH-LTD (a) and SH-LTD (b) estimated by Monta Carlo random sampling of the threshold number of ice core records (shadings); and the relative distribution of conversion factors obtained from model simulation and bomb test (Table 1).

4 Conclusions

The existing volcanic reconstructions commonly rely on the Pinatubo-based conversion factor to estimate the radiative forcing of historical volcanic eruptions. This study revisits the conversion factor, using a large collection of polar ice core records of Tambora deposition and a Monte Carlo sampling model. Uncertainties associated with the LTD factor and its applicability to the volcanic forcing reconstruction are examined, by both across-methodology-comparison between the ice core-based estimation and multi-model simulations, and across-event-comparison among Tambora, Pinatubo, Agung volcanic aerosols, and bomb test debris.

The resulting LTD_T is $1.08 \pm 0.056 \times 10^9$ km^2 for Greenland and $1.29 \pm 0.066 \times 10^9$ km^2 for Antarctic, respectively. The mean NH-LTD_T value is slightly larger than L_p used in the GRA08 reconstruction (Gao et al., 2008). The mean SH-LTD_T value is roughly a quarter larger than L_p, but in close agreement with factor used in the eVolve2K reconstruction (Toohey and Sigl, 2017). This is the first set of LTD conversion factor that are based on consistent methodology and the most comprehensive collection of ice core observations. It also contains uncertain range estimated from Monte Carlo sampling, and corrects the bias of over-representing the west Antarctic in our previous Pinatubo-based LTD estimation.

We repeat the LTD_T calculation with Monte Carlo sampling of various number of ice core records, and the resulted mean LTD_T differ by less than 2% for varying ice core sampling size while the uncertainties, represented by the standard deviation, reduced from 32% to 10% when the sampled ice core number increases from 8 to 18 in Greenland, or from 21% to 10% as we increase the ice core number from 14 to 24 in Antarctic (Table 1). Conventionally we are prone to use as much ice core observations as available to estimate the icecap volcanic deposition and then calculate the stratospheric loading to icecap deposition conversion factor. But the Monte Carlo simulation results suggest that 15-20 records with good spatial coverage is likely to be representative. It is more important to build a distribution of the conversion factor.

The comparison of SH-LTD among Tambora, Agung, and Pinatubo suggests that, the conversion factor may vary for individual eruption depending on the eruptive characteristic and magnitude as well as the volcano location. This magnitude-induced variation is also simulated by the MAECHAM5-HAM model (Toohey et al., 2013), albeit only matters for eruptions larger than Tambora. It is important to acknowledge that none LTD from a single eruption could probably represent all the eruptions. Nevertheless, the estimated sets of Tambora-based conversion factors (LTD_T) could serve as a compromising choice in future volcanic forcing reconstruction work, especially when Tambora is utilized as a reference.

Acknowledgments and Data Availability

The work is supported by the National Natural Science Foundation of China (41875092). We sincerely thank all the colleagues who drilled the ice cores and generated the original volcanic signal data, without whom this work and our previous works on volcanic forcing reconstruction would not be possible. We also appreciate the anonymous reviewers for their constructive comments and suggestions which helped to improve the paper.

The supplementary dataset and information are accessible at http://www.geodoi.ac.cn (Gao C C and Gao Y, 2020, DOI: 10.3974/geodb.2020.07.07.V1).

References

Ammann, C. M., Meehl, G. A., Washington, W. M., & Zender, C. S. (2003). A monthly and latitudinally varying volcanic forcing dataset in simulations of 20th century climate. *Geophysical Research Letters*, *30*, 1657. https://doi:10.1029/2003GL016875.

Bigler, M., Wagenbach, D., Fischer, H., Kipfstuhl, J., Millar, H., Sommer, S., & Stauffer, B. (2002). Sulphate record from a Northeast Greenland ice core over the last 1200 years based on continuous flow analysis. *Annals of Glaciology, 35*, 250-256. https://doi:10.3189/172756402781817158.

Bennett, B. (2002). Worldwide dispersion and deposition of radionuclides produced in atmospheric tests. *Health Physics, 82*, 644-655. https://doi:10.1097/00004032-200205000-00011.

Bronnimann, S., Franke, J., Nussbaumer, S. U., Zumbuhl, H. J., Steiner, D., Trachsel, M., Hegerl, G. C., Schurer, A., Worni, M., Malik, A., Flückiger, J., & Raible, C. C. (2019). Last phase of the Little Ice Age forced by volcanic eruptions. *Nature Geoscience*, *12*, 650-656. https://doi.org/10.1038/s41561-019-0402-y.

Budner, D., & Cole-Dai, J. H. (2003). The number and magnitude of large explosive volcanic eruptions between 904 and 1865 A.D.: Quantitative evidence from a new south pole ice core, in Volcanism and the Earth's Atmosphere, edited by A. Robock and C. Oppenheimer, pp. 165–176, AGU, Washington, D. C. https://doi.org/10.1029/139GM10.

Clausen, H. B., & Hammer, C. U. (1988). The Laki and Tambora eruptions as revealed in Greenland ice cores from 11 locations. *Annals of Glaciology, 10*, 16-22. https://doi.org/10.1017/S0260305500004092.

Cole-Dai, J. H., Mosley-Thompson, E., & Thomason, L. (1997). Annually resolved Southern Hemisphere volcanic history from two Antarctic ice cores, *Journal of Geophysical Research*, *102(D14), 16*, 761-771. https://doi:10.1029/97JD01394.

Cole-Dai, J., & Mosley-Thompson, E. (1999). The Pinatubo eruption in South Pole snow and its potential value to ice-core paleovolcanic records. *Annals of Glaciology*, *29*, 99-105. https://doi.org/10.3189/172756499781821319.

Cole-Dai, J. H., Mosley-Thompson, E., & Thomason, L. (2000). A 4100-year record of explosive volcanism from an East Antarctica ice core, *Journal of Geophysical Research*, *105(D19)*, *24*, 431– 24,441. https://doi:10.1029/2000JD900254.

Crowley, T. J. (2000). Causes of climate change over the past 1000 years. *Science*, *289*, 270–277. https://doi:10.1126/science.289.5477.270.

Dixon, D., Mayewski, P. A., Kaspari, S., Sneed, S., & Handley, M. (2004). A 200 year sub-annual record of sulfate in West Antarctica, from 16 ice cores, *Annals of Glaciology*, *39*, 545– 556. https://doi:10.3189/172756404781814113.

Delmas, R. J., Kirchner, S., Palais, T. M., & Petit, J. R. (1992). 1000 years of explosive volcanism recorded at the South-Pole, *Tellus B*, *44(4)*, 335–350. https://doi:10.1034/j.1600-0889.1992.00011.x.

Gao, C., Oman, L., Robock, A., & Stenchikov, G. L. (2007). Atmospheric volcanic loading derived from bipolar ice cores accounting for the spatial distribution of volcanic deposition. *Journal of Geophysical Research*, *112*, D09109. https://doi:10.1029/2006JD007461.

Gao, C. C., Gao, Y. J., Zhang, Q., & Shi, C. H. (2017). Climatic aftermath of the 1815 Tambora eruption in China. *Journal of Meteorological Research*, *31*, 28–38. https://doi:10.1007/s13351-017-6091-9.

Gao, C. C., & Gao, Y. (2020). Dataset of Ice Core Deposition to Stratospheric

Loading Conversion Factor and the Tropical Volcanic Forcing of the Past 1500 Years (2.0). *Global Change Data Repository*. https://doi:10.3974/geodb.2020.07.07.V1.

Gautier, E., Savarino, J., Erbland, J., Lanciki, A., & Possenti, P. (2016). Variability of sulfate signal in ice-core records based on five replicate cores. *Climate of the Past*, *12*, 103-113. https://doi:10.5194/cp-12-103-2016.

Gertisser, R., Self, S., Thomas L. E., Handley H. K., Calsteren P. V., & Wolff, J., A. (2012). Processes and timescales of magma genesis and differentiation leading to the great Tambora eruption in 1815. *Journal of Petrology*. *53*, 271–297. https://doi:10.1093/petrology/egr062.

Jiang, S. et al. (2012). A detailed 2840 year record of explosive volcanism in a shallow ice core from Dome A, East Antarctica. *Journal of Glaciology*, *58*, 65-75. https://doi:10.3189/2012JoG11J138.

Luterbacher, J., & Pfister, C. (2015). The year without a summer. *Nature Geoscience*, *8*, 246–248. https://doi: 10.1038/ngeo2404.

Legrand, M., & Delmas, R. (1987). A 220 year continuous record of volcanic H_2SO_4 in the Antarctic ice sheet, *Nature*, *327*, 671 – 676. https://doi:10.1038/327671a0.

Marshall, L., Schmidt, A., Toohey, M., Carslaw, K. S., Mann, G. W., Sigl, M., Khodri, M., Timmreck, C., Zanchettin, D., Ball, W. T., Bekki, S., Brooke, J. S. A., Dhomse, S., Johnson, C., Lamarque, J.-F., LeGrande, A. N., Mills, M. J., Niemeier, U., Pope, J. O., Poulain, V., Robock, A., Rozanov, E., Stenke, A., Sukhodolov, T., Tilmes, S., Tsigaridis, K., & Tummon, F. (2018). Multi-model comparison of the volcanic sulfate deposition from the 1815 eruption of Mt. Tambora. *Atmospheric Chemistry & Physics*, *18*, 2307–2328. https://doi.org/10.5194/acp-18-2307-2018.

Mosley-Thompson, Thompson, E., L. G., Dai, J., Davis, M., & Lin, P. N. (1993). Climate of the last 500 years: High-resolution ice core records, *Quaternary Science Reviews*, *12(6)*, 419–430. https://doi:10.1016/S0277-3791 (05)80006-X.

Mosley-Thompson, E., Mashiotta, T. A., & Thompson, L. (2003). High resolution ice core records of late Holocene volcanism: Current and future contributions from the Greenland PARCA cores. *Volcanism and the Earth's Atmosphere*, *139*, 153–164. https://doi.org/10.1029/139GM09.

Mayewski, P. A., Lyons, W. B., Spencer, M. J., Twickler, M. S., Buck, C. F., & Whitlow, S. (1990). An ice-core record of atmospheric response to anthropogenic sulfate and nitrate, *Nature*, *346*, 554– 556. https://doi:10.1038/346554a0.

Mayewski, P. A., Twickler, M.S., Whitlow, S.I., Meeker, L.D., Yang Q., Thomas J., Kreut, K., Grootes, P.M., Morse, D.L., Steig, E.J., Waddington, E.D., Saltzman, E.S., Whung, P.Y., & Taylor, K.C. (1996). Climate change during the last deglaciation in Antarctica. *Science*, *272*, 1636-1638. https://doi:10.1126/science.272.5268.1636.

Moore, J. C., Narita, H., & Maeno, N. (1991). A continuous 770-year record of volcanic activity from East Antarctica, *Journal of Geophysical Research*, 96(D9), 17, 353–359, https://doi:10.1029/91JD01283.

Motizuki, M., Nakai, Y., Takahashi, K., Igarashi, M., Motoyama, H., & Suzuki, K. (2014). Dating of a Dome Fuji (Antarctica) shallow ice core by volcanic signal synchronization with B32 and EDML1 chronologies. *The Cryosphere Discuss*, *8*, 769-804. https://doi.org/10.5194/tcd-8-769-2014.

Peterson, K. R. (1970). An empirical model for estimating world-wide deposition from atmospheric nuclear detonations. *Health Physics*, *18*, 357-378. https://doi.org/10.1097/00004032-197004000-00007.

Pinglot, J. F., & Pourchet, M. (1995). Radioactivity measurements applied to glaciers and lake sediments. *Science of the Total Environment*, *173*, 211-223. https://doi.org/10.1016/0048-9697 (95)04779-4.

Pourchet, M., Magand, O., Frezzotti, M., Ekaykin, A., & Winther, J. G. (2003). Radionuclides deposition over Antarctica. *Journal of Environmental Radioactivity*, *68*, 137-158. https://doi.org/10.1016/S0265-931X (03)00055-9.

Palmer, A. S., Morgan, V. L., Curran, A. J., Van Ommen T. D., & Mayewski, P. A. (2002). Antarctic volcanic flux ratios from Law Dome ice cores, *Annals of Glaciology*, *35*, 329–332. https://doi:10.3189/172756402781816771

Pinto, J. P., Toon, O. B., and Turco, R. P. (1989). Self-limiting physical and chemical effects in volcanic eruption clouds. *Journal of Geophysical Research*, *94*, 11165–11174, https://doi.org/10.1029/JD094iD08p11165

Raible, C. C., Brönnimann, S., Auchmann, R., Auchmann, R., Brohan, P., Frölicher, T. L., Graf, H-F., Jones, P., Luterbacher, J., Muthers, S., Neukom, R., Robock, A., Self, S., Sudrajat, A., Timmreck, C., & Wegmann, M. (2016). Tambora 1815 as a test case for high impact volcanic eruptions: Earth system effects. *WIRs: Climate Change*, *7*, 569–589. https://doi.org/10.1002/wcc.407.

Sato, M., Hansen, J. E., M., McCormick, M. P., & Pollack, J. B. (1993). Stratospheric aerosol optical depths, 1850–1990. *Journal of Geophysical Research*, *98*, 987–22,994. https://doi:10.1029/93JD02553.

Self, S., Gertisser, R., Thordarson, T., Rampino, M. R., & Wolff, J. A. (2004). Magma volume, volatile emissions, and stratospheric aerosols from the 1815 eruption of Tambora. *Geophysical Research Letters*, *31*, L20608. https://doi.org/10.1029/2004GL020925.

Self, S. and King, A. J. (1996). Petrology and sulfur and chlorine emissions of the 1963 eruption of Gunung Agung, Bali, Indonesia. *Bulletin of Volcanology*, *58*, 263-285. https://doi.org/10.1007/s004450050139.

Sigl, M., McConnell, J. R., Layman, L., Maselli, O., McGwire, K., Pasteris, D., Dahl-Jensen, D., Steffensen, J. P., Vinther, B., Edwards, R., Mulvaney, R., & Kipfstuhl, S. (2013). A new bipolar ice core record of volcanism from WAIS Divide and NEEM and implications for climate forcing of the last 2000 years. *Journal of Geophysical Research: Atmospheres*, *118*, 1151–1169. https://doi.org/10.1029/2012JD018603.

Sigl, M., McConnell, J. R., Toohey, M., Curran, M., Das, S. B., Edwards, R., Isaksson, E., Kawamura, K., Kipfstuhl, S., Krüger, K., Layman, L., Maselli, O. J., Motizuki, Y., Motoyama, H., Pasteris, D. R., & Severi, M. (2014). Insights from Antarctica on volcanic forcing during the Common Era. *Nature Climate. Change*, *4*, 693–697. https://doi.org/10.1038/nclimate2293.

Sigl, M., Winstrup, M., McConnell, J. R., Welten, K. C., Plunkett, G., Ludlow, F., Büntgen, U., Caffee, M., Chellman, N., Dahl-Jensen, D., Fischer, H., Kipfstuhl, S., Kostick, C., Maselli, O. J., Mekhaldi, F., Mulvaney, R., Muscheler, R., Pasteris, D. R., Pilcher, J. R., Salzer, M., Schüpbach, S., Steffensen, J. P., Vinther, B. M., & Woodruff, T. E. (2015). Timing and climate forcing of volcanic eruptions for the past 2,500 years. *Nature*, *523*, 543–549. https://doi.org/10.1038/nature14565.

Stenni, B., Proposito, M., Gragnani, R., Flora, O., Jouzel, J., Falourd, S., & Frezzotti, M. (2002). Eight centuries of volcanic signal and climate change at Talos Dome (East Antarctica). *Journal of Geophysical Research*, *107(D9)*, 4076. https://doi:10.1029/2000JD000317.

Toohey, M., Kruger, K., & Timmreck, C. (2013). Volcanic sulfate deposition to Greenland and Antarctica: A modeling sensitivity study. *Journal of Geophysical Research*, *118*, 4788-4800. https://doi.org/10.1002/jgrd.50428.

Toohey, M., & Sigl, M. (2017). Volcanic stratospheric sulfur injections and aerosol optical depth from 500 BCE to 1900 CE. *Earth System Science Data*, *9*, 809-831. https://doi.org/10.5194/essd-9-809-2017.

Traufetter, F., Oerter, H., Fischer, H., Weller, R., & Miller, H. (2004). Spatiotemporal variability in volcanic sulphate deposition over the past 2kyr in snow pits and firn cores from Amundsenisen. *Journal of Glaciology*, *50*, 137–146. https://doi:10.3189/172756504781830222.

Zielinski, G. A. (1995). Stratospheric loading and optical depth estimates of explosive volcanism over the last 2100 years derived from the Greenland-Ice-Sheet-Project-2 ice core. *Journal of Geophysical Research*, *100*, 937-955. https://doi.org/10.1029/95JD01751.

Table 1.

Stratospheric volcanic aerosol loading to ice cap deposition conversion factors for tropical eruptions obtained in different studies (data also available in the supplementary dataset DOI: 10.3974/geodb.2020.07.07.V1; Gao C C and Gao Y, 2020)**.**

Method	**For tropical eruptions based on Greenland ice cores ($\times 10^9$ km^2)**	**For tropical eruptions based on Antarctic ice cores ($\times 10^9$ km^2)**	**Reference**
Ice-core-based estimations			
Bomb test calculation ($L_{\beta-1982}$)	1.0-2.75		Clausen & Hammer (1988)
	2.4		Zielinski (1995)
Bomb test calculation ($L_{\beta-2000}$)	0.76-1.0		Gao et al. (2007)
Pinatubo observation (L_p)		1.0	Gao et al. (2007)
		1.27-2.0[a]	Toohey & Sigl (2017)
Updated Pinatubo observation (LTD_p)		1.67±0.09	This study
Agung observarion (LTD_A)		0.92±0.04	This study
Tambora observation (LTD_T)	**1.08±0.056**	**1.29±0.066**	**This study**
[c]Model simulations			
GISS Pinatubo (L_{GISS})	0.46	0.46	Gao et al. (2007)
GISS Tambora (L_{GISS})	0.55	0.55	Gao et al. (2007)
CESM1-WACCM Tambora	0.31	1.63	Marshall et al (2018)
MEACHAM5-HAM Tambora	0.19	0.19	Toohey et al. (2013); Marshall et al. (2018)
SOCOL-AER Tambora	0.22	0.34	Marshall et al. (2018)
UM-UKCA Tambora	0.97	2.91	Marshall et al. (2018)
4 model average (BTD_T)	**0.42**	**1.27**	**Marshall et al. (2018)**

[a] The values are obtained by multiplying the original sulfate conversion factor of 1.2±0.3 km^2 by the factor 4/3, in order to scale the conversion factor from volcanic sulfate to sulfate aerosol.

[b] The 8 Greenland ice core records include three (Camp Century，North Central，and Dye 3) that have both Tambora and total β activities signals, and five (NorthGRIP, GISP2, Greenland SiteT, 18C, and 20D) that are in close-by locations to the cores that have total β activities.

[c] The four models used in Marshall et al. (2018) are coupled chemistry-climate models with chemical process and resolutions both superior to GISS model E, the obtained conversion factor is called Burden-to-deposition (BTD) factors.

Table 2.

Sulfate depositions for the 1815 Tambora eruption in the 25 Greenland ice cores (data also available in the supplementary dataset DOI: 10.3974/geodb.2020.07.07.V1; Gao C C and Gao Y, 2020)**.**

Ice core sites	**Latitude (°N)**	**Longitude (°W)**	**accumulation rate (m)**	**Tambora Dep. (kg km^{-2})**	**Reference**	**Original source**
Camp Century	77.18	61.11	0.35	63	Clausen & Hammer (1988)	/
North Central	74.62	39.60	0.132	48	Clausen & Hammer (1988)	/
Créte	71.12	37.32	0.267	53	Clausen & Hammer (1988)	/
Site A	70.63	35.82	0.282	41	Clausen & Hammer (1988)	/
Site B	70.65	37.48	0.301	71	Clausen & Hammer (1988)	/
Site D	70.64	39.62	0.336	129	Clausen & Hammer (1988)	/
Site E	71.76	35.85	0.207	13	Clausen & Hammer (1988)	/
Site G	71.15	35.84	0.231	94	Clausen & Hammer (1988)	/
Dye 3	65.18	43.83	0.5	54	Clausen & Hammer (1988)	/
4 B	65.17	43.93	N/A	98	Clausen & Hammer (1988)	/
18 C	65.03	44.39	N/A	25	Clausen & Hammer (1988)	/
Dye 2	66.48	46.33	0.344	N/A	Clausen & Hammer (1988)	/
NGTb20	79	36.5	0.098	25	Mosley-Thompson et al. (2003)	/
NASA-U	73.8	49.5	0.333	N/A	Mosley-Thompson et al. (2003)	/
Greenland site T	72.5	38.5	0.224	38	Mosley-Thompson et al. (2003)	/
D2	71.8	46.2	0.424	52	Mosley-Thompson et al. (2003)	/
D3	69.8	44	0.488	85	Mosley-Thompson et al. (2003)	/
Raven	65.9	46.3	0.325	55	Mosley-Thompson et al. (2003)	/
Humboldt	78.5	56.8	0.142	N/A	Mosley-Thompson et al. (2003)	/
North GRIP	75	43	0.152	37	Gao et al. (2007)	Bigler et al. (2002)
GISP2	72.6	38.5	0.42	73	Gao et al. (2007)	Zielinski, G. A. (1995)
Greenland site A	70.8	36	0.267	27	Gao et al. (2007)	Mosley-Thompson et al.(1993)
20D	65	45	0.41	85	Gao et al. (2007)	Mayewski et al, (1990)
Tunu2013	78	33.9	0.1	18	Sigl et al. (2015)	/
NEEM2011S1	77.5	51.1	0.21	47.25	Sigl et al. (2013)	/

Table 3.
Sulfate depositions for the tropical eruptions of 1815 Tambora, 1963 Agung, and 1991 Pinatubo in the 33 Antarctic ice cores (data also available in the supplementary dataset DOI: 10.3974/geodb.2020.07.07.V1; Gao C C and Gao Y, 2020)**.**

Ice core sites	Latitude (° S)	Longitude (° E)	accumulation rate (m)	Tambora Dep. (kg km^{-2})	Agung Dep. (kg km^{-2})	Pinatubo Dep. (kg km^{-2})	Reference	Original source
Law Dome	66.7	112.8	0.644	65	14	14	Gao et al. (2007)	Palmer et al. (2002)
Dyer	70.7	64.9	0.45	87	12	N/A	Gao et al. (2007)	Cole-Dai et al. (1997)
G15	71	46	0.13	88	N/A	N/A	Gao et al. (2007)	Moore et al. (1991)
Talos Dome	72.8	159.1	0.081	38	3	N/A	Gao et al. (2007)	Stenni et al. (2002)
Herc Neve	73.1	165.5	0.119	19	N/A	N/A	Gao et al. (2007)	Stenni et al. (2002)
Dome C	74.7	124.2	0.031	8	8	N/A	Gao et al. (2007)	Legrand & Delmas(1987)
DMLb32	75	0	0.061	28	N/A	12	Gao et al. (2007)	Traufetter et al. (2004)
Siple Station	76	-84.3	0.55	118	29	N/A	Gao et al. (2007)	Cole-Dai et al. (1997)
ITASE015	77.1	-89.1	0.389	65	22	20	Gao et al. (2007)	Dixon et al. (2004)
ITASE005	77.7	-124	0.136	61	11	8	Gao et al. (2007)	Dixon et al. (2004)
ITASE004	78.1	-120.1	0.19	76	10	14	Gao et al. (2007)	Dixon et al. (2004)
ITASE013	78.1	-95.6	0.326	N/A	15	10	Gao et al. (2007)	Dixon et al. (2004)
ITASE001	79.4	-111.2	0.218	73	7	15	Gao et al. (2007)	Dixon et al. (2004)
ITASE991	80.6	-122.6	0.13	63	15	15	Gao et al. (2007)	Dixon et al. (2004)
Plateau Rm	84	43	0.04	20	8	N/A	Gao et al. (2007)	Cole-Dai et al. (2000)
SP2001c1	89	0	0.08	61	8	3	Gao et al. (2007)	Budner & Cole-Dai(2003)
SP95	89	0	0.078	60	10	N/A	Gao et al. (2007)	Dixon et al. (2004)
PS1	89	0	0.08	68	0	N/A	Gao et al. (2007)	Delmas et al. (1992)
PS14	89	0	0.08	61	8	N/A	Gao et al. (2007)	Delmas et al. (1992)
DML05	75	0	0.062	28	N/A	11	Sigl et al. (2015)	Traufetter et al. (2004)
B40	75	0	0.068	32	8	6	Sigl et al. (2015)	/
DML07	75.6	3.4	0.059	41	7	3	Sigl et al. (2015)	Traufetter et al. (2004)
NUS08-5	75.6	3.4	0.037	35	7	3	Sigl et al. (2015)	/
NUS07-2	76.2	22.5	0.033	13	N/A	N/A	Sigl et al. (2015)	/
DF01	77.4	39.7	0.027	29	N/A	N/A	Sigl et al. (2015)	Motizuki et al. (2014)
DFS10	77.4	39.6	0.027	44	8	7	Sigl et al. (2015)	/
Taylor Dome	78	159	0.1	19	N/A	N/A	Sigl et al. (2015)	Mayewski et al. (1996)
NUS07-5	78.7	35.6	0.024	28	4	N/A	Sigl et al. (2015)	/
WDC06A	79.5	-112.1	0.21	78	13	15	Sigl et al. (2013)	/
WDC05Q	79.5	-112.1	0.21	86	15	12	Sigl et al. (2013)	/
DA2005	80.4	77.2	0.023	53	N/A	N/A	Sigl et al. (2015)	Jiang, S et al (2012)
NUS07-7	82.1	54.9	0.03	9	19	3	Sigl et al. (2015)	/
NUS08-4	82.8	19.8	0.036	17	12	5	Sigl et al. (2015)	/

Table 4. Distribution statistics of the LTD factors of Tambora using Monta Carlo random sampling of selected number of ice core records. The convergence rate is defined as the change in the range of μ±σ per increase of ice core number.

Greenland;	**8 (36%)**		**10 (45%)**		**12 (55%)**		**14 (64%)**		**16 (73%)**		**18 (82%)**	
Tambora	**60Tg**	**80Tg**	**60Tg**	**80Tg**	**60Tg**	**80Tg**	**60Tg**	**80Tg**	**60Tg**	**80Tg**	**60Tg**	**80Tg**
Mean ($\times 10^9$ km^2)	1.097	1.475	1.089	1.464	1.086	1.460	1.082	1.454	1.079	1.451	1.077	1.448
Standard deviation	0.166	0.223	0.135	0.182	0.111	0.149	0.091	0.123	0.075	0.100	0.056	0.075
Convergence rate	NaN		0.031	0.041	0.024	0.033	0.020	0.026	0.016	0.023	0.019	0.025
Skewness	0.72		0.68		0.56		0.53		0.55		0.51	
kurtosis	0.63		0.54		0.27		0.21		0.17		0.01	
Antarctica: Tambora	**14 (44%)**		**16 (50%)**		**18 (56%)**		**20 (63%)**		**22 (69%)**		**24 (75%)**	
Mean ($\times 10^9$ km^2)	1.308	1.758	1.302	1.750	1.299	1.747	1.296	1.743	1.297	1.743	1.294	1.740
Standard deviation	0.138	0.186	0.118	0.159	0.101	0.136	0.089	0.120	0.077	0.103	0.066	0.089
Convergence rate	NaN		0.020	0.027	0.017	0.023	0.012	0.016	0.012	0.017	0.011	0.014
Skewness	0.97		0.65		0.47		0.49		0.38		0.46	
kurtosis	3.49		1.49		0.55		0.72		0.13		0.22	

[a] The results are obtained by assuming that the Agung eruption injected 7Mt of SO_2 into the stratosphere (Self and King, 1996) and all converted to sulfate aerosols. Then 2/3 of the Agung aerosols, i.e. 9.5 Mt of sulfate aerosols, is partitioned into the Southern Hemispheric stratosphere.

Table 5.

Distribution statistics of the LTD factors of Pinatubo and Agung using Monta Carlo random sampling of selected number of ice core records. The convergence rate is defined as the change in the range of μ±σ per increase of ice core number.

Antarctica: Agung	**10 (42%)**	**12 (50%)**	**14 (58%)**	**16 (67%)**	**18 (75%)**	**20(83%)**
Mean (×10^9 km^2)	0.94	0.93	0.93	0.93	0.93	0.92
Standard deviation	0.11	0.09	0.08	0.06	0.05	0.04
Convergence rate	NaN	0.02	0.01	0.02	0.01	0.01
Skewness	0.54	0.41	0.44	0.44	0.51	0.53
kurtosis	0.44	-0.01	0.03	0.00	0.10	0.02
Antarctica: Pinatubo	**6 (33%)**	**8 (44%)**	**10 (56%)**	**12 (67%)**	**14 (78%)**	**16 (89%)**
Mean (×10^9 km^2)	1.77	1.71	1.69	1.68	1.67	1.67
Standard deviation	0.44	0.30	0.23	0.18	0.13	0.09
Convergence rate	NaN	0.14	0.07	0.05	0.05	0.04
Skewness	1.42	0.90	0.81	0.77	0.75	0.76
kurtosis	5.40	0.93	1.02	1.17	1.09	0.58

Figure 1.

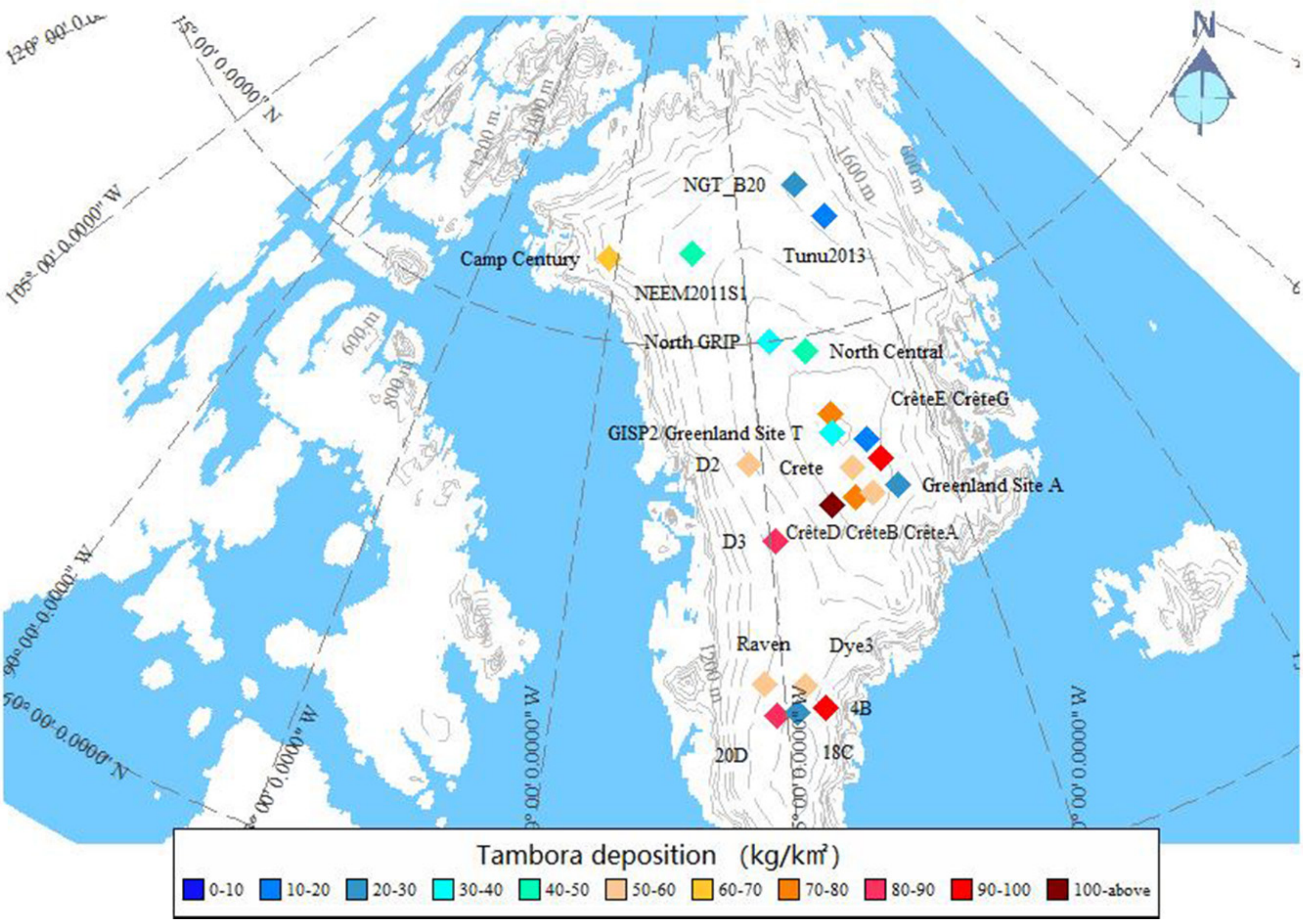

N
NGT_B20
Tunu2013
Camp Century
NEEM2011S1
North GRIP
North Central
CrêteE/CrêteG
GISP2/Greenland Site T
D2
Crete
Greenland Site A
CrêteD/CrêteB/CrêteA
D3
Raven
Dye3
4B
20D
18C
1600 m
600 m
800 m
1200 m
Tambora deposition (kg/km²)
0-10
10-20
20-30
30-40
40-50
50-60
60-70
70-80
80-90
90-100
100-above

Figure 2.

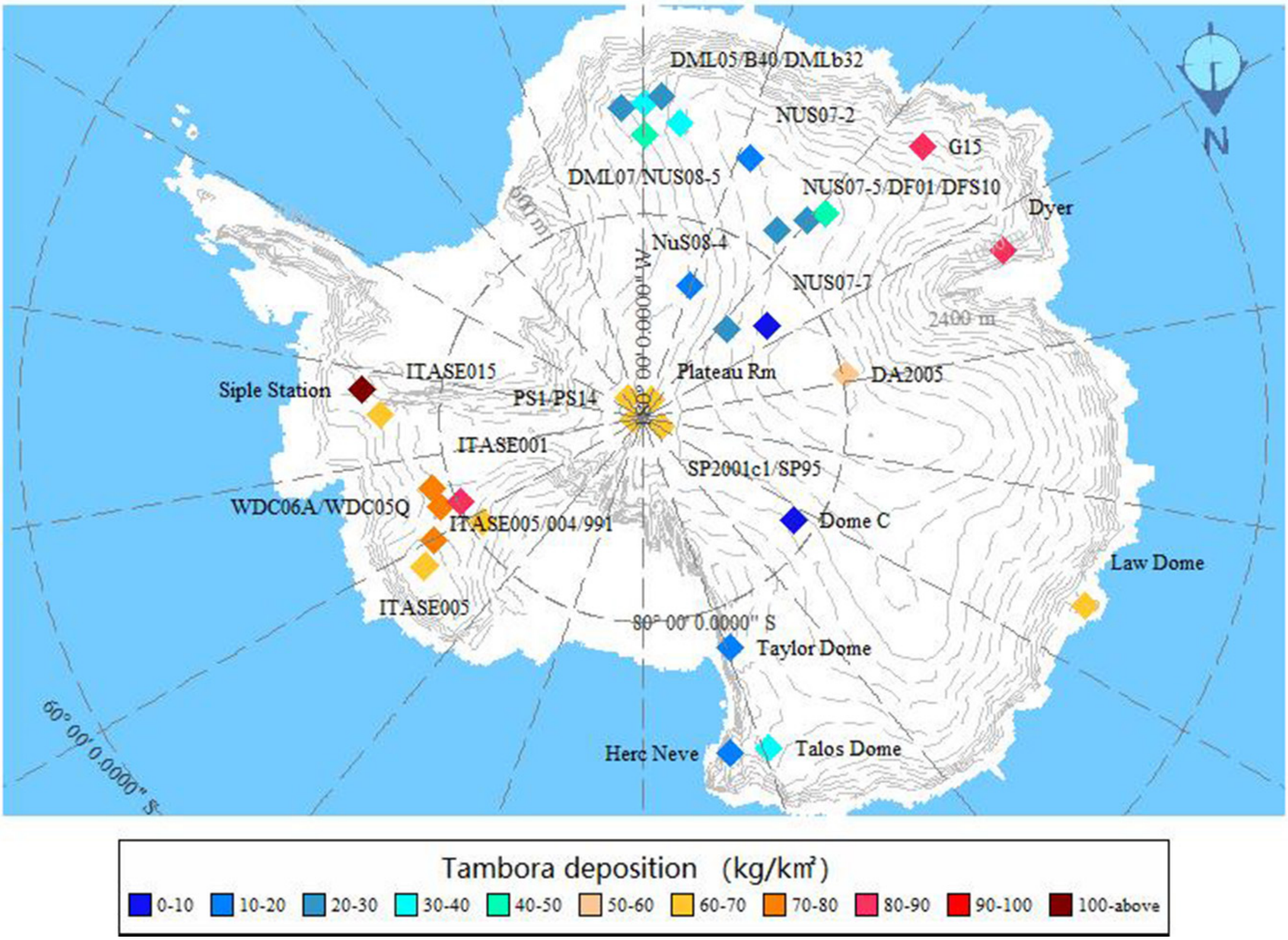
DML05/B40/DMLb32
NUS07-2
G15
DML07/NUS08-5
NUS07-5/DF01/DFS10
Dyer
NuS08-4
NUS07-7
2400 m
Plateau Rm
DA2005
ITASE015
Siple Station
PS1-PS14
ITASE001
SP2001c1/SP95
WDC06A/WDC05Q
ITASE005/004/991
Dome C
Law Dome
ITASE005
80° 00' 0.0000'' S
Taylor Dome
60° 00' 0.0000'' S
Herc Neve
Talos Dome
N
Tambora deposition (kg/km²)
0-10
10-20
20-30
30-40
40-50
50-60
60-70
70-80
80-90
90-100
100-above

Figure 3.

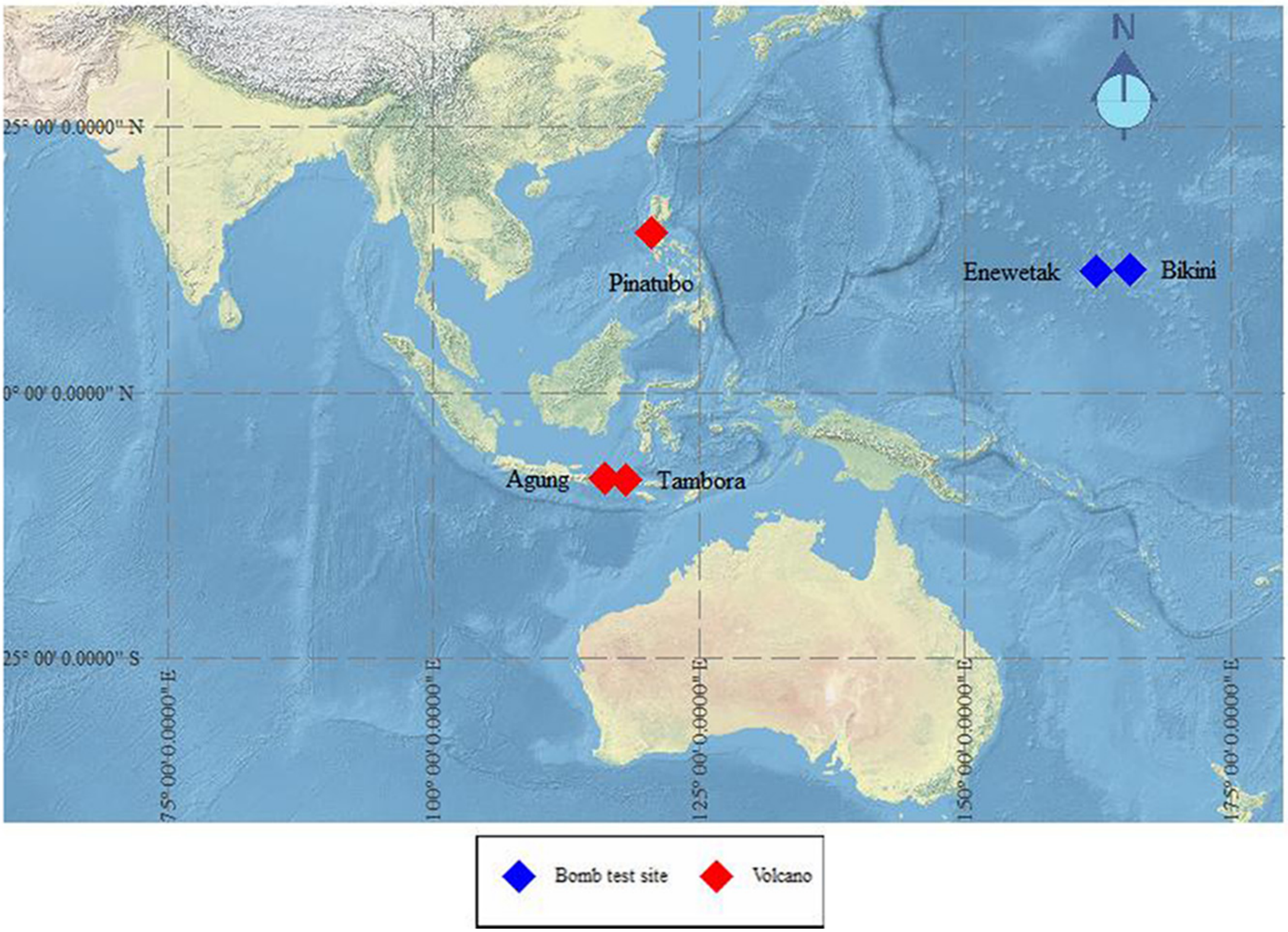
N
25° 00' 0.0000'' N
0° 00' 0.0000'' N
25° 00' 0.0000'' S
75° 00' 0.0000'' E
100° 00' 0.0000'' E
125° 00' 0.0000'' E
150° 00' 0.0000'' E
175° 00' 0.0000'' E
Pinatubo
Enewetak
Bikini
Agung
Tambora
Bomb test site
Volcano

Figure 4.


a
b
c
d
Occurrence Probability
Cumulative Probability
Distribution range of NH-LTD$_T$ (60Tg)
Distribution range of SH-LTD$_T$ (60Tg)
8
10
12
14
16
18
20
22
24
0.00
0.01
0.02
0.03
0.04
0.05
0.06
0.07
0.08
0.09
0.10
0.20
0.30
0.40
0.50
0.60
0.70
0.80
0.90
1.00
1.10
1.20
1.30
1.40
1.50
1.60
1.70
1.80
1.90
2.00
2.10
2.20
2.30
2.40
2.50

Figure 5.

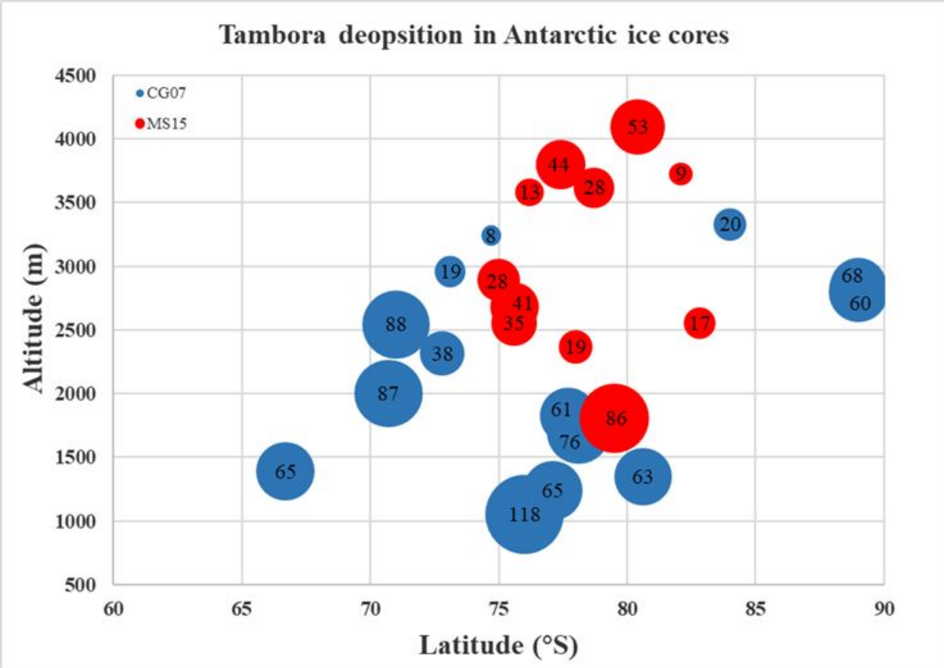
Tambora deopsition in Antarctic ice cores
CG07
MS15
Altitude (m)
Latitude (°S)
4500
4000
3500
3000
2500
2000
1500
1000
500
60
65
70
75
80
85
90
53
44
9
13
28
20
8
19
28
68
41
60
88
35
17
38
19
87
61
86
76
65
63
65
118

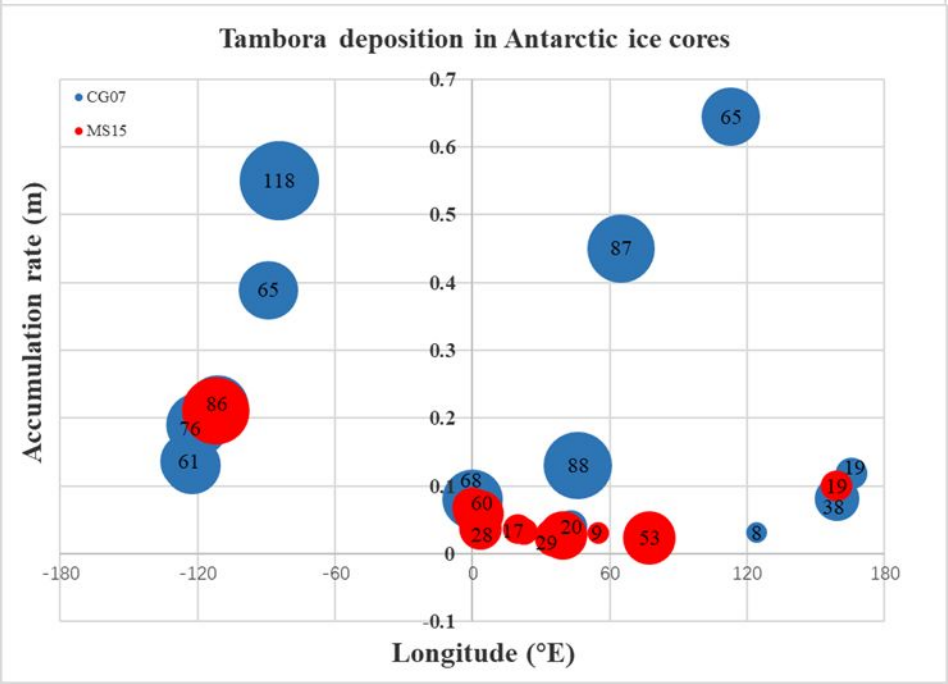
Tambora deposition in Antarctic ice cores
CG07
MS15
Accumulation rate (m)
Longitude (°E)
0.7
0.6
0.5
0.4
0.3
0.2
0.1
0
-0.1
-180
-120
-60
0
60
120
180
65
118
87
65
86
76
61
88
19
68
19
60
38
28
17
20
9
29
53
8

Figure 6.

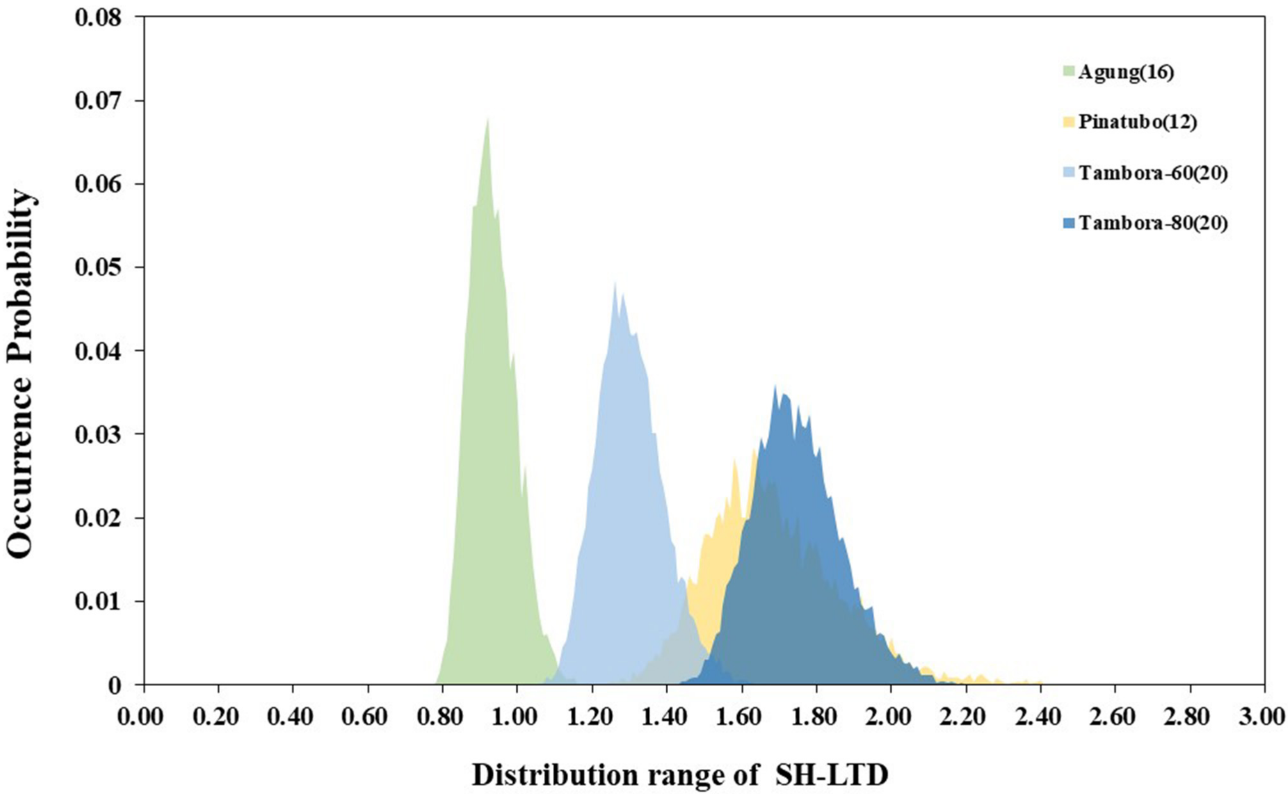

0.08
0.07
0.06
0.05
0.04
0.03
0.02
0.01
0
Occurrence Probability
Agung(16)
Pinatubo(12)
Tambora-60(20)
Tambora-80(20)
0.00
0.20
0.40
0.60
0.80
1.00
1.20
1.40
1.60
1.80
2.00
2.20
2.40
2.60
2.80
3.00
Distribution range of SH-LTD

Figure 7.

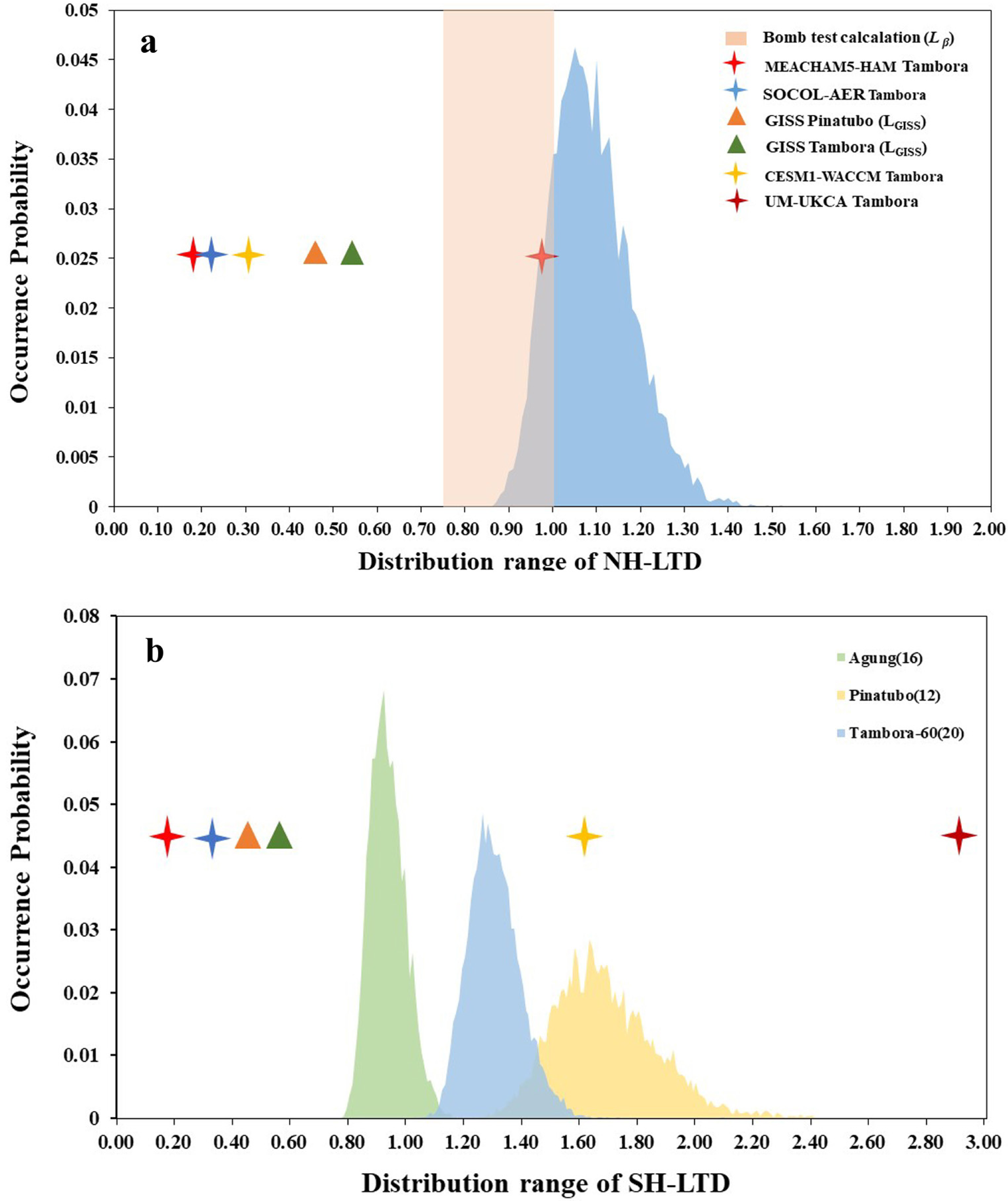
a
Bomb test calcalation (L_β)
MEACHAM5-HAM Tambora
SOCOL-AER Tambora
GISS Pinatubo (L_{GISS})
GISS Tambora (L_{GISS})
CESM1-WACCM Tambora
UM-UKCA Tambora
Occurrence Probability
0
0.005
0.01
0.015
0.02
0.025
0.03
0.035
0.04
0.045
0.05
0.00 0.10 0.20 0.30 0.40 0.50 0.60 0.70 0.80 0.90 1.00 1.10 1.20 1.30 1.40 1.50 1.60 1.70 1.80 1.90 2.00
Distribution range of NH-LTD
b
Agung(16)
Pinatubo(12)
Tambora-60(20)
Occurrence Probability
0
0.01
0.02
0.03
0.04
0.05
0.06
0.07
0.08
0.00 0.20 0.40 0.60 0.80 1.00 1.20 1.40 1.60 1.80 2.00 2.20 2.40 2.60 2.80 3.00
Distribution range of SH-LTD